

## UC Irvine

### UC Irvine Previously Published Works

**Title**

A Comparative Analysis of the Effector Role of Redox Partner Binding in Bacterial P450s.

**Permalink**

<https://escholarship.org/uc/item/50c1g11r>

**Journal**

Biochemistry, 55(47)

**Authors**

Batabyal, Dipanwita  
Lewis-Ballester, Ariel  
Yeh, Syun-Ru  
[et al.](#)

**Publication Date**

2016-11-29

**DOI**

10.1021/acs.biochem.6b00913

Peer reviewed



Published in final edited form as:

*Biochemistry*. 2016 November 29; 55(47): 6517–6523. doi:10.1021/acs.biochem.6b00913.

## A Comparative Analysis of the Effector Role of Redox Partner Binding in Bacterial P450s

Dipanwita Batabyal<sup>†</sup>, Ariel Lewis-Ballester<sup>‡</sup>, Syun-Ru Yeh<sup>‡</sup>, and Thomas L. Poulos<sup>\*†</sup>

<sup>†</sup>Departments of Molecular Biology and Biochemistry, Chemistry, and Pharmaceutical Sciences, University of California, Irvine, California 92697, United States

<sup>‡</sup>Department of Physiology and Biophysics, Albert Einstein College of Medicine, 1300 Morris Park Avenue, Bronx, New York 10461, United States

### Abstract

The camphor monooxygenase, cytochrome P450cam, exhibits a strict requirement for its own redox partner, putidaredoxin (Pdx), a two-iron–sulfur ferredoxin. The closest homologue to P450cam, CYP101D1, is structurally very similar, uses a similar redox partner, and exhibits nearly identical enzymatic properties in the monooxygenation of camphor to give the same single 5-*exo*-hydroxy camphor product. However, CYP101D1 does not strictly require its own ferredoxin (Arx) for activity because Pdx can support CYP101D1 catalysis but Arx cannot support P450cam catalysis. We have further examined the differences between these two P450s by determining the effect of spin equilibrium, redox properties, and stability of oxygen complexes. We find that Arx shifts the spin state equilibrium toward high-spin, which is the opposite of the effect of Pdx on P450cam. In both P450s, redox partner binding destabilizes the oxy–P450 complex but this effect is much weaker with CYP101D1. In addition, resonance Raman data show that structural perturbations observed in P450cam upon addition of Pdx are absent in CYP101D1. These data indicate that Arx does not play the same effector role in catalysis as Pdx does with P450cam. The most relevant structural difference between these two P450s centers on a catalytically important Asp residue required for proton-coupled electron transfer. We postulate that with P450cam larger Pdx-assisted motions are required to free this Asp for catalysis while the smaller number of restrictions in CYP101D1 precludes the need for redox partner-assisted structural changes.

### Graphical Abstract

\*Corresponding Author: poulos@uci.edu. Phone: 949-824-7020.

#### Author Contributions

D.B. and A.L.-B. contributed equally to this work.

#### ORCID

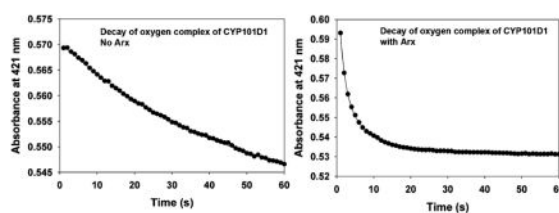
Thomas L. Poulos: 0000-0002-5648-3510

#### Notes

The authors declare no competing financial interest.

#### Supporting Information

The Supporting Information is available free of charge on the ACS Publications website at DOI: 10.1021/acs.biochem.6b00913. UV/visible spectra of CYP101D1 and Arx associated with redox potential measurements (PDF)



Cytochromes P450 (CYPs) represent one of Nature's largest enzyme families and catalyze a wide range of monooxygenation reactions. The CYP101A1 (P450cam) camphor monooxygenase system has served as the primary model for addressing structural and enzymatic aspects of CYP function. The CYP reaction cycle requires two electron transfer steps. The first reduces the heme iron from  $\text{Fe}^{3+}$  to  $\text{Fe}^{2+}$  that allows the formation of the  $\text{Fe}^{2+}\text{-O}_2$  complex. The second electron transfer step results in cleavage of the  $\text{O}_2\text{-O-O}$  bond and formation of Compound I species,  $\text{Fe}^{4+}=\text{O}$ . Like many CYPs, the P450cam redox partner is an  $\text{Fe}_2\text{S}_2$  ferredoxin called putidaredoxin (Pdx). While many CYPs can utilize various nonnative redox partners, P450cam strictly requires its own redox partner, Pdx, for the second electron transfer step.<sup>1</sup> This strict requirement for Pdx suggested early on that in addition to providing electrons to P450cam, Pdx serves an effector role by binding to P450cam and promoting structural changes required for  $\text{O}_2$  activation.<sup>1-5</sup> One of the more important observations is that Pdx shifts the P450cam-substrate complex from high-spin to low-spin,<sup>6</sup> which is associated with a shift from a closed structure to a more open structure where water has access to the active site that then can coordinate the heme iron to give a low-spin complex.

Recent crystal structures of the P450cam-Pdx complex show P450cam to be in the open conformation (Figure 1),<sup>7,8</sup> while double electron-electron resonance studies also show that Pdx shifts P450cam to the open form.<sup>9</sup> In addition, recent molecular dynamics simulations and direct binding assays using isothermal titration calorimetry show that Pdx binds more tightly to substrate-free (open) P450cam than to substrate-bound (closed) P450cam.<sup>10</sup> An important part of the open-closed transition involves the essential and highly conserved Asp251; various lines of evidence indicate that Asp251 forms part of the proton relay network required to protonate the ironlinked  $\text{O}_2$  molecule<sup>11</sup> and thus is important in the second proton-coupled electron transfer event. However, Asp251 is tied up by Arg186 and Lys178 salt bridges, which must break for Asp251 to shuttle protons into the active site. In the open form, Asp251 is free to serve its role in proton transfer, and thus, the effector role of Pdx may be to open this region of P450cam, thereby arming the proton-coupled electron transfer machinery.<sup>7</sup>

An important question is how common or unusual this complex effector role of redox partner binding is. The closest homologue to P450cam is CYP101D1, whose structure, redox partners, and enzymatic activity are very similar to those of P450cam.<sup>12-14</sup> Indeed, CYP101D1 hydroxylates camphor at the same rate and efficiency to give the same single product, 5-*exo*-hydroxy-camphor. Despite these structural and functional similarities, there are important differences. CYP101D1 has relaxed redox partner selectivity. CYP101D1 can use Pdx to support catalysis, but P450cam cannot use the CYP101D1 redox partner,

Arx.<sup>12,13</sup> In addition, while camphor shifts P450cam to 100% high-spin, camphor results in only 45–50% high-spin, yet CYP101 is as active and as tightly coupled as P450cam.<sup>12,13</sup>

In this communication, we further probe the differences between CYP101D1 and P450cam by determining the effect of redox partner binding on the spin equilibrium, the redox properties of CYP101D1, and the stability of the oxygen complex in the presence and absence of the redox partner.

## MATERIALS AND METHODS

### UV/Vis Spectroscopic Measurements

UV/vis spectra were recorded at room temperature using a UV2401 spectrophotometer (Shimadzu Scientific Instruments, Inc., Columbia, MD). The proteins were prepared in 50 mM Tris buffer (pH 7.4) containing 150 mM NaCl. The camphor-bound samples were generated with 1 mM camphor. The concentrations of CYP101D1 and Arx were 50  $\mu\text{M}$  each. After addition of either camphor or Arx, the protein samples were allowed to sit for 10–15 min at room temperature before spectra were recorded.

### Resonance Raman Spectroscopic Measurements

Resonance Raman measurements with a spectral resolution of  $1\text{ cm}^{-1}$  were performed as described previously.<sup>15</sup> Briefly, the 413.1 nm output from a Kr ion laser (Spectra Physics, Mountain View, CA) was focused to an  $\sim 30\ \mu\text{m}$  spot on a spinning quartz cell ( $\sim 6000$  rpm). The scattered light was collected at a  $90^\circ$  angle and focused on the  $100\ \mu\text{m}$  wide slit of a 1.25 m Spex spectrometer equipped with a 1200 grooves/mm grating (Horiba Jobin Yvon, Edison, NJ), where it was dispersed and detected by a CCD detector (Princeton Instruments, Trenton, NJ). Rayleigh scattering was removed by a holographic notch filter (Kaiser, Ann Arbor, MI). The Raman shifts were calibrated by using indene. The laser power was kept at  $\sim 5$  mW. The concentrations of CYP101D1 and Arx were 50  $\mu\text{M}$  each.

### Reduction Potential Measurements

The midpoint potentials of CYP101D1 and Arx were measured by monitoring the electron distribution between each protein and a dye as a function of dithionite concentration at  $25^\circ\text{C}$ . The concentrations of CYP101D1 and Arx were 12.5 and 54  $\mu\text{M}$ , respectively. Neutral red ( $-325$  mV vs SHE) and Nile blue A ( $-116$  mV vs SHE) were used for substrate-free and camphor-bound CYP101D1, respectively, while phenosafranin ( $-252$  mV vs SHE) was used for Arx.<sup>16</sup> The reaction mixture, containing each protein and dye, was loaded into a sealed cuvette, purged with nitrogen gas, and then titrated with dithionite under anaerobic conditions. The redox reaction following each addition of dithionite was allowed to reach equilibrium ( $\sim 6$  min) and then monitored using UV/vis spectroscopy (Figure S1). The ratio of the oxidized and reduced protein (or dye) was determined by the absorbance change at the isosbestic point of the dye (or protein) (Figure S2). Linear Nernst plots of the one-electron reduction reaction of the proteins and the two-electron reduction reaction of the dyes were used to estimate the redox potential of the proteins. All of the potentials cited in this work are referenced to the standard hydrogen electrode (SHE).

## Stopped Flow Experiment

Formation and decay of the oxygen complex were observed using an SX.18MV stopped flow apparatus from Applied Photophysics at 23 °C. Briefly, ferric CYP101D1 in buffer [50 mM potassium phosphate (pH 7.4) and 1 mM D-camphor] was first degassed and purged with nitrogen and then reduced inside a glovebox (anaerobic chamber) by careful titration with a 5 mM sodium dithionite stock (in the same buffer). Stopped flow syringes were washed first with a 5 mM sodium dithionite solution to remove oxygen followed by washing with degassed and nitrogen-purged buffer [50 mM potassium phosphate (pH 7.4) and 1 mM D-camphor] to wash away the dithionite. In the first part of the experiment, reduced ferrous CYP101D1 in 50 mM potassium phosphate (pH 7.4) and 1 mM D-camphor was mixed with the same air-saturated buffer to form the oxy complex. In the second part of the experiment, the reduced ferrous CYP101D1 was mixed with air-saturated buffer that also now contained a 2-fold excess of oxidized Arx to compare the stability of the oxygen complex in the presence Arx. The final concentrations of CYP101D1 and Arx after mixing in the stopped flow were around 5.5 and 11  $\mu\text{M}$ , respectively. Data were fitted using Sigma Plot.

## Single-Turnover Experiments

With P450cam, the addition of oxidized Pdx to oxy-P450cam results in the formation of 0.5 equiv of product.<sup>1</sup> Similar experiments were performed with CYP101D. Oxidized Arx (40  $\mu\text{M}$ ) was added to 20  $\mu\text{M}$  oxy-CYP101D1 in a total volume of 1.5 mL. After 30 min, the solution was extracted with 750  $\mu\text{L}$  of dichloromethane and analyzed by GCT Premier (TOF from Waters) as previously described.<sup>14</sup>

## RESULTS AND DISCUSSION

### Optical Absorption Spectroscopy

A characteristic spectral feature of P450s upon substrate binding is a shift in the UV/vis spectrum from  $\approx 416$  to  $\approx 392$  nm, which is due to a change from a hexacoordinate low-spin form to a pentacoordinate high-spin form, respectively. Substrate-bound P450cam and CYP101D1 differ in that P450cam is 100% high-spin while CYP101D1 is only 45–55% high-spin even at saturating levels of camphor.<sup>12,13</sup> With P450cam, it is now well established that the low-spin state has a more open structure where water has ready access to the active site, including coordination to the heme iron, while substrate binding results in a significant structural change that closes the active site to form tight protein substrate interactions. Only the closed state structure of CYP101D1 is available, although the open state of the closely related CYP101D2<sup>17</sup> is known and the motions involved in the open–closed transition are likely to be similar in all these P450s.

Because the binding of Pdx to P450cam increases the fraction of the low-spin state, we anticipated that the binding of Arx to CYP101D1 might lead to a similar change. Instead, however, we found just the opposite. Arx shifts the CYP101D1 UV/vis spectrum more toward the high-spin form (Figure 2). Because resonance Raman spectroscopy is exquisitely sensitive to spin state changes, we next determined the effect of Arx on the RR properties of CYP101D1.

## Resonance Raman (RR) Spectroscopy

The high-frequency RR spectra of the ferric CYP101D1 are shown in Figure 3A. In the substrate-free spectrum, the  $\nu_2$  and  $\nu_3$  modes at 1583 and 1502  $\text{cm}^{-1}$ , respectively, indicate a low-spin species. The addition of Arx does not introduce any spectral changes in the absence of substrate. The addition of camphor induces the appearance of the 1487  $\text{cm}^{-1}$  band, indicating the presence of a high-spin species. The addition of Arx in the presence of camphor leads to an enhanced population of the high-spin species, consistent with the UV/vis results. This is in sharp contrast to P450cam for which RR spectroscopy shows that the P450cam redox partner, Pdx, increases the population of low-spin heme.<sup>6</sup>

The low-frequency RR spectra are shown in Figure 3B. They provide important information regarding the conformation of the porphyrin ring and the peripheral groups attached to it, including the propionate and vinyl groups, as well as the strength and geometry of the iron–ligand bond(s). The  $\delta_{\text{propionate}}$  and  $\delta_{\text{vinyl}}$  modes of the substrate-free enzyme are identified at 378/389 and 422  $\text{cm}^{-1}$ , respectively. The mode at 511  $\text{cm}^{-1}$  is tentatively assigned to the  $\nu_{\text{Fe-OH}}$  mode, as camphor binding diminishes its intensity; in addition, the same mode has been identified in P450cam at a similar position.<sup>18,19</sup> Camphor and/or Arx binding only slightly perturbs the spectrum, indicating that substrate or redox partner binding does not introduce any major conformational changes into the heme. This sharply contrasts to the case for P450cam, in which camphor binding not only induces the change in the coordination and spin state of the heme but also perturbs the  $\delta_{\text{vinyl}}$  and  $\delta_{\text{propionate}}$  modes, as well as several heme modes characteristic of distorted heme,<sup>18,19</sup> manifesting the conformational changes to the porphyrin macrocycle and the peripheral heme groups. Furthermore, in P450cam, the high-spin ferric heme is typically associated with characteristic high relative intensity ratios of  $\nu_{15}/\nu_7$ , as well as  $\nu_3/\nu_2$ , both of which are not observed in CYP101D1. Thus, the RR data presented here clearly indicate that the structural perturbations observed in P450cam upon addition of Pdx are absent in CYP101D1, further supporting the view that the redox partner Arx does not have an effector role for CYP101D1 that is as pronounced. This also is consistent with the observations that P450cam strictly requires its own redox partner for catalysis,<sup>1</sup> while CYP101D1 catalysis can be supported by Pdx, the P450cam redox partner.<sup>12,13</sup>

A simple model of the CYP101D1–Arx complex based on the P450cam–Pdx crystal structure clearly shows that the intermolecular interactions must be quite given (Figure 1). Although Arx and Pdx exhibit an only 0.8 Å root-mean-square difference in backbone atoms, the surface that interacts with the CYP is quite different (Figure 1). Particularly noteworthy is the fact that Asp38 in Pdx is Leu39 in Arx. Asp38 is located at the center of the P450cam–Pdx interface where it forms an ion pair with a P450cam Arg residue. The C-terminus in Pdx is essential for activity;<sup>20,21</sup> Arx is one residue shorter, so the C-terminal end of Arx must interact quite differently, if at all, with CYP101D1. The fact that Pdx can support CYP101D1 catalysis despite such large differences between Arx and Pdx underscores the fact that CYP101D1 is quite promiscuous with respect to its redox partner.

## Redox Potential Measurements

The midpoint potential of the P450 enzyme typically lies between  $-400$  and  $-300$  mV, which is much more negative than that of its redox partner. It is well-known that the coordination and spin state transition induced by substrate binding lead to an increase in the midpoint potential of the heme. This makes it thermodynamically favorable to accept an electron from its redox partner, thereby triggering oxygen binding and subsequent chemistry.<sup>22</sup> Our spectroscopic data show that in CYP101D1 substrate binding does not induce a complete low-spin to high-spin transition. It therefore is important to determine the effect of substrate binding on the midpoint potential. The midpoint potentials were examined by monitoring the electron distribution between the protein and a dye, with a well-defined potential,<sup>16</sup> as a function of reduction by dithionite. The concentrations of the reduced and oxidized protein (dye) were determined at an isosbestic point of the reduced and oxidized dye (protein), using optical absorption spectroscopy as described in Materials and Methods. The resulting Nerst plots of the data are shown in Figure 4. The midpoint potential of the substrate-free CYP101D1 is estimated to be  $-339$  mV (empty black circles), which is similar to that reported for P450cam ( $-303$  mV).<sup>22</sup> Binding of camphor leads to a  $+200$  mV increase in the midpoint potential to  $-139$  mV (filled black circles), similar to the substrate-induced change in P450cam (from  $-303$  to  $-173$  mV). A comparable study of Arx shows a midpoint potential of  $-220$  mV (empty gray circles in Figure 3), demonstrating that electron transfer from Arx to only high-spin CYP101D1 is thermodynamically favorable.

## Stability of the Oxygen Complex of CYP101D1

The oxy complex of P450cam in the presence of camphor is very stable ( $t_{1/2} \approx 25$ – $30$  min at  $4$  °C). Addition of Pdx to the oxy complex in the presence of camphor led to a large  $\sim 150$ -fold decrease in the stability of the oxy complex.<sup>23</sup> Given that the effect of Arx on the spin shift of CYP101D1 was the opposite of the effect of Pdx on P450cam, we wanted to compare its effect on the stability and decay of the oxygen complex in the presence of camphor.

Decay of the CYP101D1–oxy complex in the absence and presence of a 2-fold excess of Arx was followed by stopped flow kinetics at  $23$  °C (Figure 5). Reduced ferrous CYP101D1 was mixed with air-saturated buffer. The spectrum of the CYP101D1–oxy complex has a Soret absorption peak at  $421$  nm and a peak in the visible region at  $556$  nm (Figure 5C, red spectrum), which is similar to that of the P450cam–oxy complex. The oxy complex is fairly stable in the absence of Arx with a decay rate of  $0.0186 \pm 0.004$  s<sup>-1</sup> (Figure 5A shows reaction for 60 s, and the inset shows the same reaction for 600 s). However, in the presence of a 2-fold excess of oxidized Arx, decay of the oxy complex is  $\sim 33$ -fold faster with a rate of  $0.60 \pm 0.005$  s<sup>-1</sup> (Figure 5B). Panels B and D of Figure 5 show the progress of the reaction within 1 min. In the presence of Arx, the decay of the oxy complex is complete, and after 1 min, the spectrum indicates a mix of low- and high-spin ferric heme, typical of CYP101D1. In the absence of Arx, the oxygen complex decays slowly to produce a spectrum (Figure 5C, black spectra) that has much larger contribution of low-spin heme. This is consistent with our previous observation that the presence of Arx enhances the contribution of the high-spin heme in CYP101D1.



Because the addition of oxidized Pdx to oxy-P450cam results in the formation of 0.5 equiv of product,<sup>1</sup> we checked to see if CYP101D1 behaves similarly. We used 20  $\mu\text{M}$  oxy-CYP101D1 and 40  $\mu\text{M}$  oxidized Arx, which gives an easily detectable amount of product using the highly sensitive gas chromatography–mass spectrometry methods that we routinely use for product analysis. However, we found no product. We also tested to see if dithionite can support product formation, but here, too, no product was detected.

### Relevance to Catalysis

CYP101D1 catalyzes exactly the same reaction as P450cam using similar redox partners, and as the work presented here shows, the redox potentials of CYP101D1 and Arx, including the increase in redox potential of CYP101D1 upon substrate binding, are very similar to those of the P450cam system. CYP101D1 thus provides an opportunity to probe the structural and functional features that may differ without compromising catalytic efficiency. One of the most unusual properties of P450cam is its strict requirement for its redox partner Pdx, which is relaxed for CYP101D1.

In earlier studies, we postulated that these differences are due to subtle structural differences around a critical Asp residue in the active site of both P450cam and CYP101D1. Asp251 has long been known to be critical for P450cam activity<sup>24</sup> and is generally thought to be important for participating in a proton relay network required for protonation and O<sub>2</sub> bond cleavage in the formation of Compound I. The corresponding Asp259 in CYP101D1 also is essential for activity.<sup>12</sup> However, the local environment surrounding the critical Asp is quite different in each P450. In P450cam, Asp251 is tied up in salt bridges with Lys178 and Arg186 so it was always difficult to understand how Asp251 could participate in a proton relay network when anchored by two salt bridging groups. However, when Pdx binds, these salt bridges are broken, thus freeing Asp251 to serve its role in proton-coupled electron transfer. In sharp contrast, Gly in CYP101D1 replaces Lys178, and thus, Asp259 in CYP101D1 is more open to solvent and has only one salt bridge with Arg188. We also found that this salt bridge is more readily broken in CYP101D1. In our attempts to crystallize substrate-free CYP101D1, we still obtained crystals with CYP101D1 in the closed state but with a glycerol molecule bound in the substrate pocket. However, the Asp259–Arg188 ion pair is broken and replaced with water molecules that bridge the two residues (Figure 6). Although we did not observe product formation when using dithionite as the reductant, there is clear evidence that X-ray-driven reduction of CYP101D1 crystals generates product but not in P450cam crystals.<sup>12</sup> Only in the P450cam–Pdx crystals where P450cam is open and the Asp251 salt bridges are broken is product formed.<sup>7</sup> These results of X-ray-driven product formation are consistent with the more open or at least looser catalytic Asp environment being associated with relaxed redox partner selectivity.

Even so, Arx may play an effector, although more modest than Pdx. Arx does destabilize the CYP101D–oxy complex by  $\approx 30$ -fold and does shift the spin equilibrium of ferric CYP101D1 toward high-spin. Whether these Arx-induced changes result in a more open CYP101D1 conformation remains unknown. However, even if Arx plays a modest effector role, this either must not be very important or is not confined to Arx alone because Pdx can support CYP101D1 catalysis and hydroxylation of substrate in crystals can be driven by X-



rays. It is most likely that the effector role of redox partner binding spans a wide range in P450s, with P450cam representing the extreme example of selectivity and CYP101D1 representing the other extreme of relaxed selectivity.

We close by speculating about why P450cam and CYP101D1 behave so differently. It is reasonable to expect that there should be some biological advantage for P450cam exhibiting such a high level of specificity. Despite the close similarities between these two CYPs, they derive from very different bacteria. P450cam is the only CYP produced by *Pseudomonas putida* and is essential for utilizing camphor as a carbon and energy source. All three P450cam redox proteins are tightly controlled on a plasmid-borne operon and are produced only when camphor is available as a carbon source. Without a high level of selectivity in the P450cam system, *P. putida* risks the wasteful consumption of reducing equivalents that would otherwise be directed toward camphor oxidation. In sharp contrast, CYP101D1 from *N. aromaticus* is one of 16 CYPs,<sup>25</sup> and therefore, CYP101D1 is not as critical to the survival of the organism. In addition, Arx is the ferredoxin that provides electrons to all CYPs in *N. aromaticus*, so a high level of redox partner selectivity is not desirable. So far, P450cam appears to be an outlier with such a sophisticated level of control. On the other hand and given that there are many thousands of P450s in Nature that have yet to be characterized, it is very likely that there are other CYPs that behave like P450cam.

## Supplementary Material

Refer to Web version on PubMed Central for supplementary material.

## Acknowledgments

### Funding

This work was supported by National Institutes of Health (NIH) Grant GM57353 (T.L.P.) and NIH Grant GM115773 and National Science Foundation Grant CHE-1404929 (S.-R.Y.).

## References

1. Lipscomb JD, Sligar SG, Namtvedt MJ, Gunsalus IC. Autooxidation and hydroxylation reactions of oxygenated cytochrome P-450cam. *J Biol Chem.* 1976; 251:1116–1124. [PubMed: 2601]
2. Poulos TL. Heme enzyme structure and function. *Chem Rev.* 2014; 114:3919–3962. [PubMed: 24400737]
3. Tyson CA, Lipscomb JD, Gunsalus IC. The role of putidaredoxin and P450cam in methylene hydroxylation. *J Biol Chem.* 1972; 247:5777–5784. [PubMed: 4341491]
4. Nagano S, Shimada H, Tarumi A, Hishiki T, Kimata-Arigo Y, Egawa T, Suematsu M, Park SY, Adachi S-i, Shiro Y, Ishimura Y. Infrared spectroscopic and mutational studies on putidaredoxin-induced conformational changes in ferrous CO-P450cam. *Biochemistry.* 2003; 42:14507–14514. [PubMed: 14661963]
5. Pochapsky SS, Pochapsky TC, Wei JW. A model for effector activity in a highly specific biological electron transfer complex: the cytochrome P450cam-putidaredoxin complex. *Biochemistry.* 2003; 42:5649–5656. [PubMed: 12741821]
6. Unno M, Christian JF, Benson DE, Gerber NC, Sligar SG, Champion PM. Resonance Raman investigations of cytochrome P450(cam) complexed with putidaredoxin. *J Am Chem Soc.* 1997; 119:6614–6620.
7. Tripathi S, Li H, Poulos TL. Structural basis for effector control and redox partner recognition in cytochrome P450. *Science.* 2013; 340:1227–1230. [PubMed: 23744947]

8. Hiruma Y, Hass MA, Kikui Y, Liu WM, Olmez B, Skinner SP, Blok A, Kloosterman A, Koteishi H, Lohr F, Schwalbe H, Nojiri M, Ubbink M. The structure of the cytochrome p450cam-putidaredoxin complex determined by paramagnetic NMR spectroscopy and crystallography. *J Mol Biol.* 2013; 425:4353–4365. [PubMed: 23856620]
9. Myers WK, Lee YT, Britt RD, Goodin DB. The conformation of P450cam in complex with putidaredoxin is dependent on oxidation state. *J Am Chem Soc.* 2013; 135:11732–11735. [PubMed: 23901883]
10. Hollingsworth SA, Batabyal D, Nguyen BD, Poulos TL. Conformational selectivity in cytochrome P450 redox partner interactions. *Proc Natl Acad Sci U S A.* 2016; 113:8723–8728. [PubMed: 27439869]
11. Gerber NS, Sligar SG. Catalytic mechanism of cytochrome P450 - evidence for a distal charge relay system. *J Am Chem Soc.* 1992; 114:8742–8743.
12. Batabyal D, Poulos TL. Crystal structures and functional characterization of wild-type CYP101D1 and its active site mutants. *Biochemistry.* 2013; 52:8898–8906. [PubMed: 24261604]
13. Yang W, Bell SG, Wang H, Zhou W, Hoskins N, Dale A, Bartlam M, Wong LL, Rao Z. Molecular characterization of a class I P450 electron transfer system from *Novosphingobium aromaticivorans* DSM12444. *J Biol Chem.* 2010; 285:27372–27384. [PubMed: 20576606]
14. Batabyal D, Li H, Poulos TL. Synergistic effects of mutations in cytochrome P450cam designed to mimic CYP101D1. *Biochemistry.* 2013; 52:5396–5402. [PubMed: 23865948]
15. Egawa T, Yeh SR. Structural and functional properties of hemoglobins from unicellular organisms as revealed by resonance Raman spectroscopy. *J Inorg Biochem.* 2005; 99:72–96. [PubMed: 15598493]
16. Fultz ML, Durst RA. Mediator compounds for the electrochemical study of biological redox systems: a compilation. *Anal Chim Acta.* 1982; 140:1–18.
17. Yang W, Bell SG, Wang H, Zhou W, Bartlam M, Wong LL, Rao Z. The structure of CYP101D2 unveils a potential path for substrate entry into the active site. *Biochem J.* 2011; 433:85–93. [PubMed: 20950270]
18. Karunakaran V, Denisov I, Sligar SG, Champion PM. Investigation of the low frequency dynamics of heme proteins: native and mutant cytochrome P450(cam) and redox partner complexes. *J Phys Chem B.* 2011; 115:5665–5677. [PubMed: 21391540]
19. Mak PJ, Kaluka D, Manyumwa ME, Zhang H, Deng T, Kincaid JR. Defining resonance Raman spectral responses to substrate binding by cytochrome P450 from *Pseudomonas putida*. *Biopolymers.* 2008; 89:1045–1053. [PubMed: 18655143]
20. Kuznetsov VY, Poulos TL, Sevrioukova IF. Putidaredoxin-to-cytochrome P450cam electron transfer: Differences between the two reductive steps required for catalysis. *Biochemistry.* 2006; 45:11934–11944. [PubMed: 17002293]
21. Sligar SG, Debrunner PG, Lipscomb JD, Namtvedt MJ, Gunsalus IC. A role of the putidaredoxin COOH-terminus in P-450cam cytochrome m hydroxylations. *Proc Natl Acad Sci U S A.* 1974; 71:3906–3910. [PubMed: 4530269]
22. Lewis DF, Hlavica P. Interactions between redox partners in various cytochrome P450 systems: functional and structural aspects. *Biochim Biophys Acta, Bioenerg.* 2000; 1460:353–374.
23. Glascock MC, Ballou DP, Dawson JH. Direct observation of a novel perturbed oxyferrous catalytic intermediate during reduced putidaredoxin-initiated turnover of cytochrome P-450-CAM: probing the effector role of putidaredoxin in catalysis. *J Biol Chem.* 2005; 280:42134–42141. [PubMed: 16115886]
24. Gerber NC, Sligar SG. A role for Asp-251 in cytochrome P-450cam oxygen activation. *J Biol Chem.* 1994; 269:4260–4266. [PubMed: 8307990]
25. Bell SG, Dale A, Rees NH, Wong LL. A cytochrome P450 class I electron transfer system from *Novosphingobium aromaticivorans*. *Appl Microbiol Biotechnol.* 2010; 86:163–175. [PubMed: 19779713]

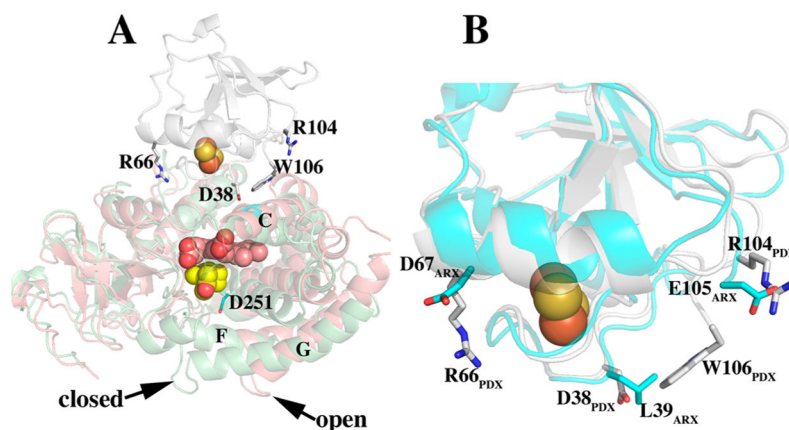


**Figure 1.** Structure of the P450cam–Pdx complex and Arx. (A) P450cam–Pdx structure [Protein Data Bank (PDB) entry 4JX1]<sup>7</sup> superimposed on the closed form of P450cam. When Pdx binds, there is a concerted motion of helix C up, while helices F and G undergo a large motion that opens up the active site and frees Asp251 to serve its function in proton-coupled electron transfer. The camphor is colored yellow, and heme is shown as pink spheres. (B) Superposition of Arx (PDB entry 3LXF)<sup>13</sup> on Pdx. Key residues in Pdx that interact with P450cam are labeled as are the corresponding residues in Arx. There is very little similarity at the binding surface indicating that the CYP101D1–Arx interface must be quite different from the P450cam–Pdx interface.

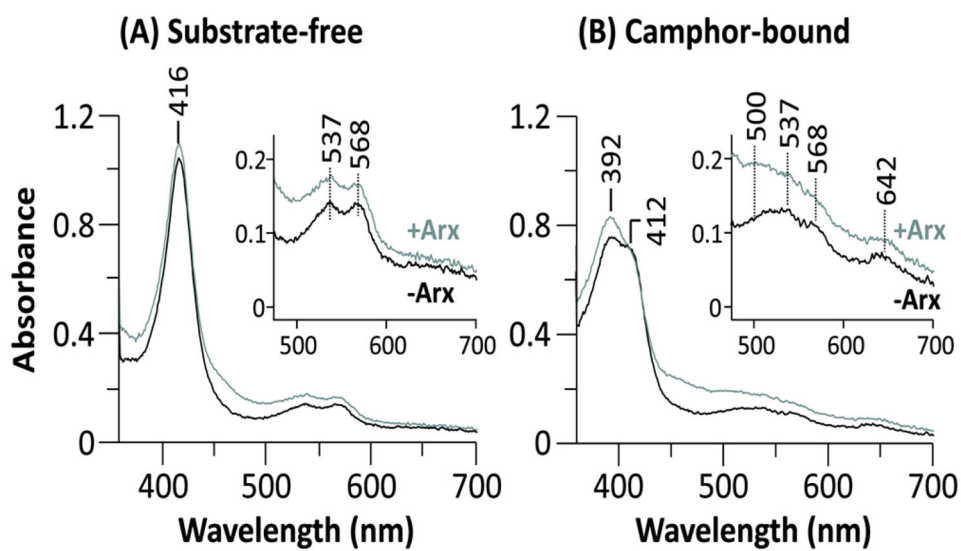


**Figure 2.** Optical absorption spectra of CYP101D1 in the absence (A) or presence of 1 mM camphor (B). The black and gray spectra were recorded in the absence and presence of the redox partner Arx, respectively.

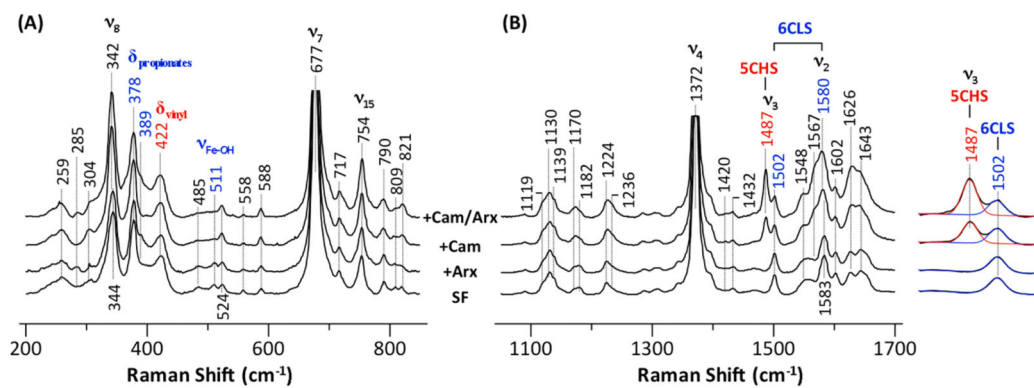


**Figure 3.** RR spectra of ferric CYP101D1 in the absence or presence of 1 mM camphor and/or the redox partner Arx. The spectra were recorded with 413.1 nm excitation.

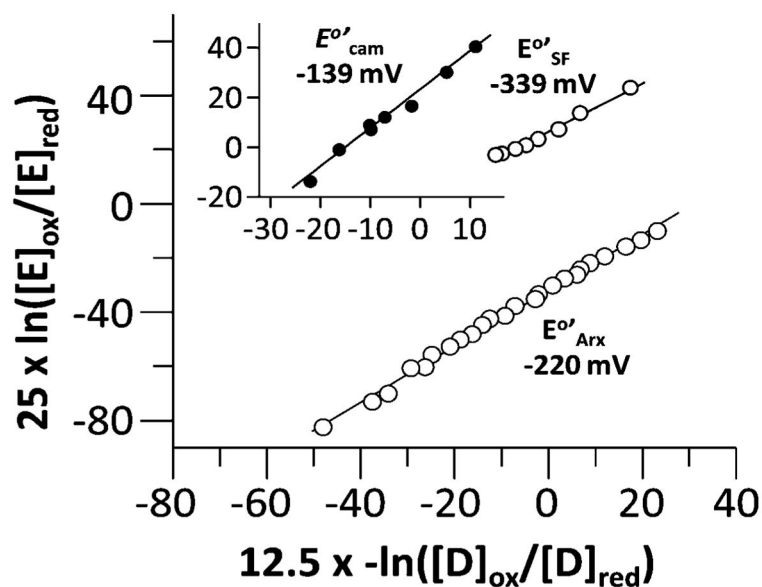


**Figure 4.** Linear Nernst plots of the redox reactions of substrate-free CYP101D1 (empty black circles), camphor-bound CYP101D1 (filled black circles), and Arx (empty gray circles). The midpoint potentials were determined by linear fits of the data based on two-electron reduction of a dye (D). The  $n$  values for the substrate-free CYP101D1 and Arx are 0.9 and 1.0, respectively, while that for the camphor-bound CYP101D1 is  $\sim 1.6$ , which deviates from unity because of the presence of some amount of substrate-free enzyme. The midpoint potential of the camphor-bound CYP101D1 was measured in the presence of 1 mM camphor.

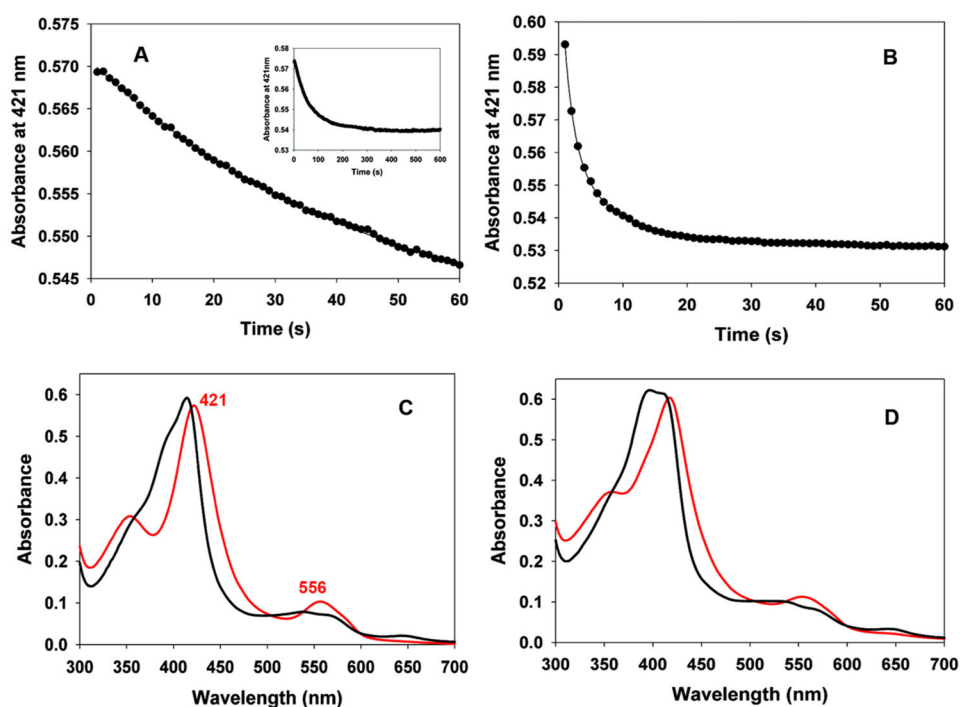


**Figure 5.** Oxy-CYP101D1. Decay of the oxy complex in the absence of Arx (A;  $k = 0.0186 \pm 0.004 \text{ s}^{-1}$ ) and in the presence of a 2-fold excess of oxidized Arx (B;  $k = 0.60 \pm 0.05 \text{ s}^{-1}$ ). Because the oxy complex is quite stable in the absence of Arx, the inset of panel A shows the same reaction for 600 s. (C) Initial spectrum (shown in red at 1 s) and final spectrum (shown in black at 600 s) in the absence of Arx. (D) Initial (shown in red at 1 s) and final (shown in black, at 1 min) spectra when reduced ferrous CYP101D1 is mixed with air-saturated buffer as observed in the stopped flow in the presence of a 2-fold excess Arx. The oxy complex is more stable in the absence of Arx but decays ~33-fold faster in the presence of Arx, forming the characteristic mixed-spin spectra for CYP101D1 in the presence of excess camphor. The buffer for all the experiments contained 50 mM potassium phosphate (pH 7.4) and 1 mM D-camphor. Reaction was conducted at room temperature (23 °C).



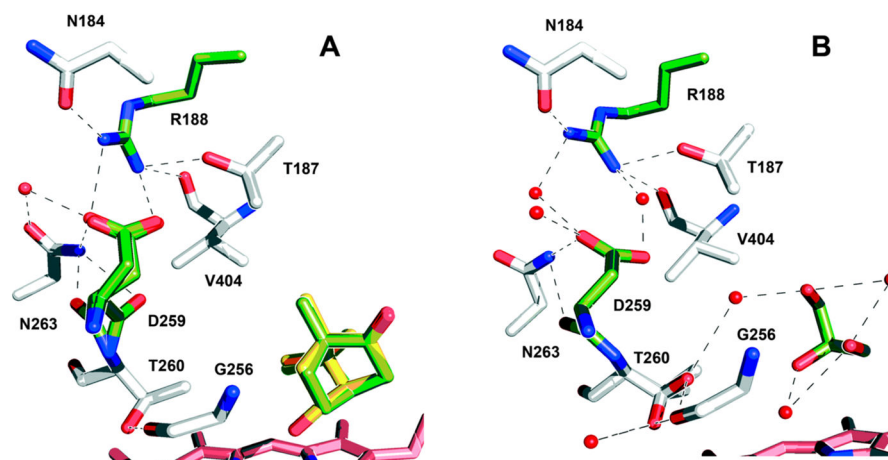


**Figure 6.** Structure of the WT CYP101D1 active site in the presence (A) and absence (B) of camphor. In panel A, the active site has camphor (and some product hydroxy camphor) bound. Asp259 and Arg188 are involved in salt bridge interactions (PDB entry 4C9K). In panel B, a glycerol molecule (green) replaces the camphor in the active site. The ion pair between Asp259 and Arg188 has been disrupted, and two new water molecules now bridge Asp259 and Arg188. Asp259, Arg188, camphor, and glycerol are colored green, and hydroxy camphor is colored yellow.